Journal of Chromatographic Science, 2019, Vol. 57, No. 4, 349–360
doi: 10.1093/chromsci/bmz006
Advance Access Publication Date: 23 February 2019
Article

Article

Comparative Metabolite Profiling of Four *Citrus* Peel Cultivars *via* Ultra-Performance Liquid Chromatography Coupled with Quadrupole-Time-of-Flight-Mass Spectrometry and Multivariate Data Analyses

Nesrin M. Fayek[1], Mohamed A. Farag[1,2], Azza R. Abdel Monem[1,*], Mohamed Y. Moussa[1], Samia M. Abd-Elwahab[1], and Nebal D. El-Tanbouly[1]

[1]Department of Pharmacognosy, Faculty of pharmacy, Cairo University, Cairo 11562, Egypt, and [2]Department of Chemistry, School of Sciences and Engineering, The American University in Cairo, New Cairo 11835, Egypt

[*]Author to whom correspondence should be addressed. Email: azzaramy@yahoo.com

Received 10 November 2017; Revised 22 October 2018; Editorial Decision 27 December 2018

Abstract

Citrus plants are one of the most economical fruit bearing trees grown worldwide for their medicinal use as well as for the flavor and food industry. This study attempts to characterize the metabolome difference in polyphenols of four *Citrus* species fruit peels; *C. reticulata* Blanco cv. Egyptian, *C. sinensis* (L.) Osbeck cv. Olinda Valencia, *C. aurantiifolia* Swingle cv. Mexican and *C. paradisi* Macfad. cv. Duncan *via* ultra-performance liquid chromatography coupled with quadrupole-time-of-flight-mass spectrometry platform. A total of 163 metabolites were characterized of which 28 were detected for the first time in *Citrus* cultivars including eight coumarin derivatives, three cinnamic acids conjugates, one polymethoxyflavone, 5 *O*-glycosides, 2 *C*-glycosides, three flavone-di-*O*-glucosides and six acetyl sugar derivatives of luteolin and kaempferol in addition to oxygenated and methylated fatty acids. Flavonoids amounted for the most abundant secondary metabolites class in the studied *Citrus* peels. The relative variability among these *Citrus* peels was estimated using clustering analysis with flavonoids accounting for cvs. segregation. Hierarchical clustering analysis revealed the chemical similarity of *C. reticulata*, *C. sinensis* and *C. paradise* peels and being distant them from that of *C. aurantiifolia.* To the best of our knowledge, this study provides the first report for metabolite compositional differences in these four *Citrus* peels.

Introduction

Metabolites profiling by mass spectrometry is considered nowadays as an emerging tool that has been increasingly applied for functional foods' analysis (1). This tool or technique involves the adoption of ultra-high performance liquid chromatography (UHPLC) coupled to high-resolution MS and can provide fast metabolite analysis with much higher sensitivity level on contrast to the conventional liquid chromatography (LC) separation (2). Such a platform has been reported to examine metabolite profiles in closely allied plant taxa, different cultivars of individual taxa or plants at various development stages (3, 4).

Citrus plants are the most economically fruit bearing plants cultivated in tropical and temperate regions (5), reaching over 123 million of tons produced during 2010 by China, Brazil, the USA and regions of the Mediterranean Basin [FAOSTAT database]. The food-processing industry of *Citrus* fruits represents 50% of the raw

processed fruit and yields considerable by-products such as peels, seeds and pulps (6). These by-products are valued as potential source for production of bioactive compounds (7), animal feed, manufactured foods and/or healthcare (8). *Citrus* fruit peels are indeed one of the most important nutraceuticals owing to their nutritional value being enriched in phenolic compounds and dietary fibers (9). A myriad of biological effects have been attributed to *Citrus* peels flavonoids including antioxidant, antimicrobial and anti-inflammatory activities (10–12). A protective effect against coronary heart disease was reported for *Citrus* phenolics acting *via* their ability to reduce plasma cholesterol concentrations mainly owing to their flavonoids content (13–17).

Metabolomics have been previously applied to forecast the free-radical scavenging activities of *Citrus* fruit (18), differentiate the pathogen resistant of *Citrus* varieties (19) and analyze orange wild-type and bud mutant fruits (20). Also, the technology has been recently used to identify novel natural product pathways in *Citrus* fruits (21), discriminate lemon essential oils from various sources (22) and investigate the differences in secondary metabolites composition among *Citrus* juices (23). More recently, metabolomics have been employed for the classification of *Citrus* species and their derived hybrids (24). To the best of our knowledge, there has been no report on classifying *Citrus* peels cultivars grown in Egypt using UPLC–MS.

In the present study, ultra-performance liquid chromatography coupled with quadrupole-time-of-flight-mass spectrometry (UPLC–qTOF–MS) based metabolomics was applied to provide a comprehensive chemical profile of the four *Citrus* peels of different genetic origins. Such large-scale profiling in *Citrus* peels could help to prioritize which cultivar ought to be more domesticated for agricultural development for its use in functional foods.

Experimental section

Plant material

Samples of the fresh fully mature ripe *Citrus* fruit peels were collected in February 2011 [for sweet orange (*C. sinensis* L. Osbeck cv. Olinda Valencia)], September 2011 [for lime (*C. aurantiifolia* Swingle cv. Mexican)], second half of December 2011 [for grapefruit (*C. paradisi* Macfad. cv. Duncan)] and second half of January 2012 [for mandarin (*C. reticulata* Blanco cv. Egyptian)], from the private orchard of El-Mazloom company for horticulture production at 78-km Cairo-Ismailia road. The plant materials were identified by Prof. Dr Mohamed El-Sayed, *Citrus* department, Horticultural Institute, Ministry of Agriculture, Giza, Egypt and voucher specimens numbers 14-7-2016-I, 14-7-2016-II, 14-7-2016-III and 14-7-2016-IV, respectively, were deposited at the Museum of the Pharmacognosy Department, Faculty of Pharmacy, Cairo University, Egypt.

Chemicals and reagents

Acetonitrile and formic acid (LC–MS grade) were purchased from J.T. Baker (the Netherlands); Milli-Q water was used for UPLC analysis. All other chemicals and standards were provided by Sigma-Aldrich (St. Louis, MO, USA).

Extraction procedure and sample preparation for UPLC–MS analysis

The dried, deep frozen *Citrus* peels were ground with a pestle in a mortar using liquid nitrogen. Then, the resulted powder (160 mg) was homogenized with 7-mL 100% MeOH containing 10-µg/mL umbelliferone (an internal standard for relative quantification using UPLC–MS) using a Turrax mixer (11,000 *g*) for 20 s for five periods. Each mixing period was separated from the next mixing period by 1 min to prevent heating. The produced MeOH extracts were then vortexed vigorously and centrifuged at 3,000 *g* for 30 min to remove plant debris and filtered through 22-µm pore size filter. The protocol reported by (25) was used as a reference for the extraction of *Citrus* specimens.

For UPLC–MS analyses, 500 µL of the methanol extract were placed on a C_{18} (500 mg) cartridge (Agilent Technologies, USA) preconditioned with methanol and water. Samples were then eluted using 6-mL methanol. The eluent was evaporated to dryness under a nitrogen stream and the obtained dry residue was re-suspended in 1-mL methanol.

High-resolution UPLC–qTOF–MS analysis

Chromatographic separations were performed, according to (26), on an Acquity UPLC system (Waters) equipped with a HSS T3 column (100 × 1.0 mm, particle size 1.8 µm; Waters) applying the following elution binary gradient at a flow rate of 150 µL min^{-1}: 0–1 min, isocratic 95% A (water/formic acid, 99.9/0.1 [v/v]), 5% B (acetonitrile/formic acid, 99.9/0.1 [v/v]); 1–16 min, linear from 5 to 95% B; 16 to 18 min, isocratic 95% B; and 18 to 20 min, isocratic 5% B. The injection volume was 3.1 µL (full loop injection). Eluted compounds were detected from m/z 100–1,000 in the negative ion mode using the following instrument settings: nebulizer gas, nitrogen, 1.6 bar; dry gas, nitrogen, 6 L min^{-1}, 190°C; capillary, −5,500 V; in-source CID energy, 0 V; hexapole RF, 100 Vpp; quadrupole ion energy, 5 eV; collision gas, argon; collision energy, 10 eV; collision RF 200/400 Vpp (timing 50/50); transfer time, 70 µs; prepulse storage, 5 µs; pulser frequency, 10 kHz; spectra rate, 3 Hz. Internal mass calibration of each analysis was performed by the infusion of 20 µL 10-mM lithium formate in isopropanol: water, 1:1 (v/v), at a gradient time of 18 min using a diverter valve. Each specimen was analyzed in triplicate.

Identification and relative quantification of metabolites and MS data multivariate analyses (HCA)

Metabolite identification was done *via* ultraviolet–visible spectroscopy (UV–VIS) spectra (220–600 nm), mass spectra and comparison with both reference literature and phytochemical dictionary of natural products database. Relative quantification and comparison of *Citrus* metabolic profile after UPLC–MS were performed using X-calibur Mass spectrometry data analysis software under R 2.9.2 environment, which can be downloaded for free as an R package from the Metlin Metabolite Database (27).

Results

Metabolite identification *via* UPLC–MS analysis

UPLC coupled with UV photodiode array detection and high-resolution qTOF mass spectrometer was employed to analyze metabolites of the four *Citrus* peels species, using a gradient mobile-phase that allowed for a comprehensive elution of analytes within *ca.* 900 s. (Figure 1). The elution order of metabolites followed a sequence of decreasing polarity, whereby phenolic acids followed by coumarins, flavonoid di-glucoside, mono-glucoside, free aglycone and fatty acids. Extracts were analyzed in negative ionization modes

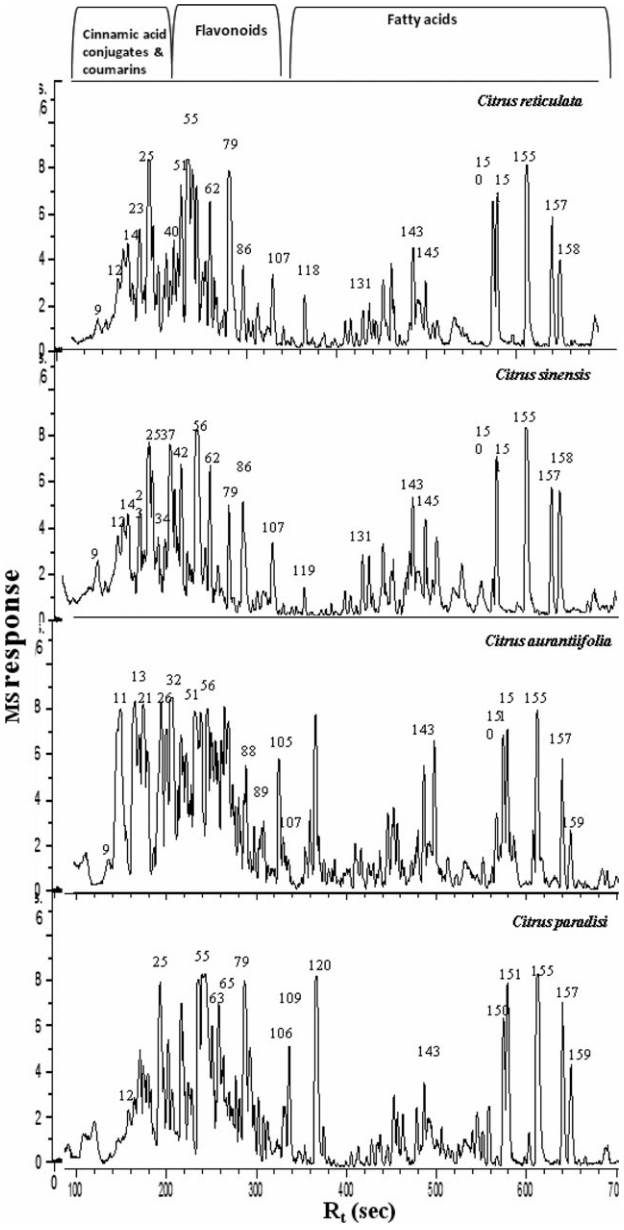

Figure 1. UPLC–qTOF–MS fingerprinting analyses of the four studied *Citrus* peels analyzed in negative ionization mode.

as *Citrus* is known to contain coumarins and flavonoids, of which the latter preferentially ionize under negative ionization condition. *Citrus* phenolics are relatively polar compounds with phenol groups in the molecules, and hence, could be easily ionized in the negative ionization mode as expected.

The selected chromatographic parameters described in the "Experimental section" resulted in the separation of 163 metabolite peaks, out of which 111 metabolites were annotated categorized into seven classes: flavonoids (40), polymethoxyflavones (7), cinnamic acid conjugates (4), coumarines (14), terpenes (7), fatty acids (32) and miscellaneous (7). Metabolites were identified based on their UV absorption spectra (200–600 nm), high-resolution qTOF mass and analysis of fragmentation patterns. Each sub-class has a characteristic UV spectrum (28), i.e., hydroxycinnamates typically have a maximum absorbance near 280 nm with a second maximum around 325 nm whereas flavonols have maximum around 340–355 nm. The retention time, characteristic molecular and fragment ions for the different components and their identities are presented in Table I. Chromatogram was divided into three regions for metabolites classes' elution including: organic acids, cinnamates and coumarins (RT 26–210 s), flavonoids (RT 211–350 s) and the last region (350–700 s) for fatty acids (Figure 1).

Hierarchical cluster analysis

Hierarchical cluster analysis (HCA) applied to the total ion current chromatogram data from the UPLC–qTOF–MS analysis, clustered samples in a fairly intuitive graphical way. The similarity or dissimilarity between the samples is presented in dendrogram depicted in Figure 2 with peels of *Citrus* samples spread into two clusters, referred as Group I (*C. aurantiifolia*) and Group II (*C. reticulata*, *C. sinensis* and *C. paradisi*) peels.

Discussion

Identification of organic acid, cinnamates and coumarins

Few organic acids, cinnamic acid conjugates and coumarins appeared in the first part of the chromatographic run (Rt 26–210 s) as revealed from their MS spectral data. Peak (2) was identified as quinic acid, with an $[M\text{-}H]^-$ at m/z 191.10 $(C_7H_{11}O_6)^-$, previously reported as the chief organic acid in *Citrus* fruit peels (29). Peak (9) exhibited $[M\text{-}H]^-$ at m/z 355.10 $(C_{15}H_{15}O_{10})^-$ and UV max at 312 nm, assigned as caffeic acid conjugate, previously reported in *Citrus* (30). Peaks (10 and 11), $[M\text{-}H]^-$ m/z 355.06 $(C_{15}H_{15}O_{10})^-$, exhibited a λ_{max} at 288 and 312–320 nm typical of coumarins (31) and were annotated as trihydroxycoumarin hexoside and its isomer (32). Peaks (12, 14 and 23) with a UV λ_{max} at 312–320 nm and $[M\text{-}H]^-$ at *m/z* 385.07 $(C_{16}H_{17}O_{11})^-$, yield fragments at m/z 223 [M-162 (hexose)-H]$^-$ and m/z 209 [M-hexose-CH_2-H]$^-$ for tetrahydroxycoumarin, assigned as methoxy-trihydroxycoumarin hexoside and its isomers. Loss of methyl group was observed in peak (18), $[M\text{-}H]^-$ m/z 369.08 $(C_{16}H_{17}O_{10})^-$, exhibiting a fragment mass at m/z 355 [M-14-H]$^-$ and sugar losses at *m/z* 207 [M-162-H]$^-$ and was identified as methoxy-umbelliferone-hexoside. Peak (25) with $[M\text{-}H]^-$ at m/z 399.09 $(C_{17}H_{19}O_{11})^-$ yielded fragments at m/z 161 [M-238-H]$^-$ for umbelliferone, m/z 205 [M-194-H]$^-$, m/z 323 for umbelliferone-hexosyl, m/z 337 [M-32-H]$^-$, m/z 369 [M-30-H]$^-$ and m/z 385 [M-14-H]$^-$, assigned as dimethoxy-umbelliferone hexoside.

The molecular ion m/z 357.11 was observed as parent ion in peak (31) $(C_{16}H_{21}O_9)^-$ and further as product ion in peak (32), $[M\text{-}H]^-$ at m/z 715.24 $(C_{32}H_{43}O_{18})^-$. Loss of hexose sugar in peak (31) at m/z 195 [M-162-H]$^-$, assists in identification of peaks (31 and 32) as dihydroxyhydrocinnamic acid hexoside and its dimer, respectively. As mentioned previously (33), the UV λ_{max} at 280 and 330 nm for peak (49), $[M\text{-}H]^-$ at m/z 501.16 $(C_{22}H_{29}O_{13})^-$, with the product ions at *m/z* 193 for ferulic acid moiety [M-308-H]$^-$ and m/z 339 [M-162-H]$^-$, assigned peak (49) as feruloyl rutinoside.

Peak (28), $[M\text{-}H]^-$ at m/z 507.20 $(C_{22}H_{35}O_{13})^-$ annotated as benzyl-methyl-cyclohexanecarboxylate-umbelliferone pentoside [Combined Chemical Dictionary] and showing a product ion for loss of sugar at m/z 375 [M-132-H]$^-$. It is worth to note that all of the above mentioned coumarin derivatives (peaks 10, 11, 12, 14, 18, 23, 25, 28) and cinnamic acid conjugates (peaks 31, 32 and 49) were detected for the first time in the examined *Citrus* peels.

Table I. Peak Assignments of Metabolites in the Four Examined *Citrus* Peels Methanol Extract *via* UPLC–PDA–qTOF–MS in Negative Ionization Mode

Peak	Rt (s)	UV (nm)	Deprotonated molecular formula	Mol. Ion $[M-H]^-$ *m/z* (-)	Error *m/z* (ppm)	MSn ions *m/z* (-) MS–MS	Identification	CR	CS	CA	CP	Class
1	24.2		$C_{12}H_{21}O_{11}$	341.1	1	179, 161	Disaccharide		*			Misc.
2	26		$C_7H_{11}O_6$	191.05	0.1	179, 165, 133	Quinic acid			*	*	Misc.
3	28.8		$C_{18}H_{17}O_9$	377.08	2.2	341, 215, 191, 179, 133	Unknown Lignan	*				Misc.
4	41.3		$C_{13}H_{17}O_{10}$	333	0.3	287, 191	Unidentified				*	
5	51.1		$C_{47}H_{39}O_{11}$	779	1.1		Unidentified				*	
6	99.2		$C_{14}H_{25}O_{10}$	353.14	2.4	311, 179	Propanol-pentosyl-hexoside			*		Misc.
7	108.6	311.3	$C_{13}H_{13}O_9$	313.05	1.1	248, 225, 191, 179, 161	Unidentified		*			
8	110.6	297, 308	$C_{14}H_{25}O_{10}$	353.14	1.1	311, 179	Propanol-pentosyl-hexoside isomer			*		Misc.
9	135.6	312 sh	$C_{15}H_{15}O_{10}$	355.06	0.7	291, 223, 209, 203, 191, 179	Caffeic acid conjugate	*	*	*		Cinn. acid
10	144.7	288, 312 sh	$C_{15}H_{15}O_{10}$	355.06	0.4	323, 313, 291, 223, 209, 203, 191, 179	Trihydroxycoumarin hexoside	*	*			Coum.
11	155.8	288, 312 sh	$C_{15}H_{15}O_{10}$	355.06	0.5	331, 313, 307, 293, 263, 233, 221, 209, 191	Trihydroxycoumarin hexoside isomer			*		Coum.
12	158.5	279 sh, 312 sh	$C_{16}H_{17}O_{11}$	385.07	0	355, 313, 293, 223, 209, 191	Methoxy-trihydroxycoumarin hexoside	*	*		*	Coum.
13	165.2		$C_{30}H_{51}O_{20}$	731.3	1.6	527, 433, 365, 355, 363	Unidentified			*		
14	169.6	312 sh	$C_{16}H_{17}O_{11}$	385.07	1.4	369, 355, 313, 293, 257, 209, 191	Methoxy-trihydroxycoumarin hexoside isomer	*	*			Coum.
15	171	318 sh	$C_{13}H_{13}O_9$	313.05	0	263, 191	Unidentified				*	
16	174.3	316	$C_{20}H_{29}O_{11}$	445.17	0	399, 385, 369, 355, 313, 293, 191	Unidentified	*	*			
17	175.3	286 sh, 318 sh	$C_{15}H_{25}O_{10}$	365.14	0.2	313, 191	Unidentified			*	*	
18	176.6	314	$C_{16}H_{17}O_{10}$	369.08	0.2	355, 313, 223, 207, 191, 193, 179	Methoxy-umbelliferone-hexoside		*			Coum.
19	177	314	$C_{16}H_{27}O_{10}$	379.16	0.8	369, 355, 313, 223, 191	Unidentified	*				
20	177.4	317 sh	$C_{22}H_{27}O_{14}$	515.14	2.5	469, 365, 313	Unidentified				*	
21	180	290 sh, 325 sh	$C_{30}H_{25}O_{10}$	545.15	11	497, 447, 433, 365, 355	Afzelechin-afzelechin			*		Misc.
22	180.4	288 sh, 323 sh	$C_{23}H_{29}O_{15}$	545.15	2.6	515, 469, 385, 365, 313	Unidentified				*	
23	182.4	320 sh	$C_{16}H_{17}O_{11}$	385.07	3.6	369, 355, 337, 313, 223, 209, 191	Methoxy-trihydroxycoumarin hexoside isomer	*	*			Coum.
24	186.8	288, 321 sh	$C_{22}H_{31}O_{14}$	519.17	0.8	497, 407, 399, 365, 337, 305, 255	Unidentified			*	*	
25	187.5	322	$C_{17}H_{19}O_{11}$	399.09	1.2	385, 369, 337, 323, 223, 205, 179, 161	Dimethoxy-umbelliferone hexoside	*	*		*	Coum.
26	191.5	268, 293 sh	$C_{18}H_{27}O_{13}$	451.14	1.4	435, 431, 407, 391, 369, 337, 209	Unidentified			*		
27	192.8	270, 328	$C_{20}H_{31}O_{10}$	431.19	1.4	399, 385	Unidentified	*	*		*	
28	200.5	284, 326	$C_{22}H_{35}O_{13}$	507.2	0.5	461, 433, 399, 375, 367, 311	Benzyl-methyl-cyclohexanecarboxylate-umbelliferone pentoside	*	*			Coum.
29	202.9	270, 291, 328	$C_{27}H_{29}O_{17}$	625.14	2.1	597, 507, 391, 375, 301	Quercetin-*O*-dihexoside	*	*			Flav.
30	203.3	270, 340 sh	$C_{17}H_{27}O_{10}$	391.16	0.2	379, 377, 369, 357, 337, 289, 277	Unidentified			*		
31	206	325 sh	$C_{16}H_{21}O_9$	357.11	1.2	195, 161	Dihydroxyhydrocinnamic acid hexoside		*			Cinn. acid
32	206.3	275	$C_{32}H_{43}O_{18}$	715.24	0.8	509, 357	Dimer of Dihydroxyhydrocinnamic acid hexoside			*		Cinn. acid
33	208.3	269, 288 sh, 321 sh	$C_{20}H_{27}O_{10}$	427.16	1.2	399, 327, 295	Unidentified				*	
34	208.7	270, 325 sh	$C_{26}H_{27}O_{15}$	579.13	3.2	489, 459, 399, 369	Luteolin-*C*-hexoside-*C*-pentoside		*			Flav.
35	209.3	270, 295, 323	$C_{20}H_{33}O_{10}$	433.2	0.5	399, 391, 333	Unidentified	*				
36	210.4	269, 328	$C_{17}H_{27}O_{10}$	391.16	0.4	377, 369, 357, 333, 289	Unidentified		*			
37	211.4	269, 325	$C_{27}H_{29}O_{15}$	593.15	3.9	509, 431, 391	Vitexin-2″-*O*-hexoside		*			Flav.

(*Continued*)

Table I. Continued

Peak	Rt (s)	UV (nm)	Deprotonated molecular formula	Mol. Ion $[M-H]^-$ *m/z* (-)	Error *m/z* (ppm)	MSn ions *m/z* (-) MS–MS	Identification	CR	CS	CA	CP	Class
38	212	268, 318	$C_{20}H_{31}O_{10}$	431.19	2.2	391, 337, 206	Unidentified	*				
39	213.7	271, 284, 316 sh	$C_{17}H_{29}O_9$	377.18	0.6	354, 327, 250, 206	Unidentified		*	*	*	
40	216.7	270, 288	$C_{26}H_{27}O_{14}$	563.14	0.9	431, 427	Vitexin-*O*-pentoside	*				Flav.
41	220.4	271, 283, 323 sh	$C_{21}H_{31}O_9$	427.19	0.6	399, 311, 295	Unidentified	*			*	
42	221.8	268, 327 sh	$C_{27}H_{29}O_{15}$	593.16	5.4	503, 473, 383, 353	Apigenin-di-*C*-hexoside {Vicenin-2}		*			Flav.
43	222.8	267, 340 sh	$C_{17}H_{23}O_{10}$	387.13	2.1	367, 225, 161	Unidentified			*		
44	224.5	272, 324	$C_{32}H_{41}O_{14}$	649.24	0.3	593, 487, 433, 387, 162, 161	Ichangin-hexoside	*				Flav.
45	224.8	323	$C_9H_5O_3$	161.02	5.5		Umbelliferone		*		*	Coum.
46	226.2	322 sh	$C_{19}H_{29}O_{11}$	433.17	1.7	399, 387, 377, 367, 161	Unidentified			*		
47	226.5	288 sh, 323 sh	$C_{27}H_{31}O_{15}$	595.16	5.3	519, 427, 287, 161	Eriocitrin {Eriodictyol-*O*-rutinoside}				*	Flav.
48	228.9	293 sh, 323	$C_{26}H_{25}O_{14}$	561.12	0.8	519, 459, 399, 367, 285, 221	Unknown flavonoid				*	Flav.
49	232.6	280 sh, 330.8 sh	$C_{22}H_{29}O_{13}$	501.16	0.5	399, 397, 357, 339, 193	Feruloyl rutinoside			*		Cinn. acid
50	232.9	320.8	$C_{18}H_{29}O_8$	373.18	2.8	291, 249, 223, 161	Unidentified		*			
51	235.6	283, 327 sh	$C_{27}H_{31}O_{14}$	579.17	1	415, 373, 271	Naringin	*	*	*		Flav.
52	238	278, 324 sh	$C_{18}H_{29}O_8$	373.18	0.8	331, 237, 221, 183, 161	Unidentified		*			
53	239	350.2 sh	$C_{19}H_{23}O_{11}$	427.12	2	417, 367, 265	Unidentified			*		
54	240.7	277, 297, 318	$C_{28}H_{31}O_{15}$	607.16	4	561, 461, 429, 373, 299	Diosmin {Diosmetin-7-*O*-neohesperidoside}		*			Flav.
55	241	283, 327 sh	$C_{27}H_{31}O_{14}$	579.17	0.1	561, 429, 271	Naringin isomer	*			*	Flav.
56	245.4	286	$C_{28}H_{33}O_{15}$	609.18	1.6	415, 301	Hesperidin{Hesperitin-*O*-rutinoside}		*	*		Flav.
57	246.7	283	$C_{28}H_{33}O_{15}$	609.18	3.7	415, 301	Hesperidin isomer		*			Flav.
58	249.7	277 sh	$C_{43}H_{23}O_3$	587.16	4.4	543, 469, 399, 195	Unidentified			*		
59	250.4	287, 318	$C_{26}H_{25}O_{14}$	561.12	0.9	531, 500, 489, 415, 367	Unknown flavonoid	*				Flav.
60	252.1	293 sh, 322	$C_{43}H_{49}O_{22}$	917.27	1	779, 579, 561, 531, 500, 489, 415, 367	Unknown flavonoid	*				Flav.
61	253.5	284, 324 sh	$C_{36}H_{43}O_{19}$	779.24	0.5	609, 579, 519, 489, 461, 429	Unidentified				*	
62	255.1	291, 323	$C_{26}H_{25}O_{14}$	561.12	0.4	531, 489, 411, 367	Unknown flavonoid	*	*			Flav.
63	256.5	284, 324	$C_{23}H_{21}O_{12}$	489.1	0.8	447, 463, 441,367, 295, 285	Luteolin-acetyl hexoside				*	Flav.
64	261.5	271.9 sh, 313 sh	$C_{48}H_{29}O_5$	685.2	3.5	409, 351, 205, 163	Unidentified			*		
65	261.6	284, 323 sh	$C_{21}H_{29}O_{10}$	441	0.2	415, 287, 279	Unknown aglycone hexoside				*	Flav.
66	263.6	283, 322	$C_{27}H_{35}O_{14}$	583.2	1.6	551, 489, 461, 457, 441	Unidentified				*	
67	265.2	270, 317 sh	$C_{49}H_{31}O_6$	715.21	3.9	685, 657, 613, 381	Unidentified			*		
68	265.3	278, 315 sh	$C_{21}H_{31}O_8$	411.2	0.9	395, 373, 221, 161	Unidentified	*	*			
69	267.3	276, 316	$C_{26}H_{25}O_{14}$	561.12	1.2	519, 489, 411, 373, 295	Unknown flavonoid	*	*			Flav.
70	267.9	287, 321	$C_{21}H_{33}O_8$	413.21	0.4	295, 263, 221	Unidentified	*				
71	269.3	340 sh	$C_{48}H_{29}O_5$	685.19	3.5	627, 459, 407, 225	Unidentified			*		
72	270	286, 323	$C_{23}H_{21}O_{12}$	489.1	0.5	447, 459, 413, 373, 395, 285	Luteolin-acetyl hexoside isomer		*		*	Flav.
73	272.3	257, 323	$C_{30}H_{37}O_{17}$	669.2	0.2	625, 579, 489, 457	Luteolin-acetyl hexoside derivative				*	Flav.
74	273	287 sh, 320	$C_{23}H_{21}O_{12}$	489.1	0.7	447, 395, 367, 295, 285	Luteolin-acetyl hexoside isomer	*	*			Flav.
75	273.7	270.4 sh, 330, 365	$C_{29}H_{31}O_{17}$	651.16	0.1	621, 609, 481, 447, 285	Kaempferol-dihexosyl acetate			*		Flav.
76	276	286, 318	$C_{14}H_{19}O_5$	267.12	1	223, 161	Unidentified	*				
77	276.7	300	$C_{33}H_{39}O_{17}$	707.22	0.4	651, 603, 481, 289, 267	Kaempferol-dihexosyl butyl acetate			*		Flav.
78	277.7	284, 318	$C_{20}H_{17}O_{10}$	417.08	1.1	327, 295, 285, 267, 251, 175	Luteolin-*C*-pentoside		*		*	Flav.

(*Continued*)

Table I. Continued

Peak	Rt (s)	UV (nm)	Deprotonated molecular formula	Mol. Ion $[M-H]^-$ *m/z* (-)	Error *m/z* (ppm)	MSn ions *m/z* (-) MS–MS	Identification	CR	CS	CA	CP	Class
79	281	283, 325 sh	$C_{29}H_{35}O_{16}$	639.19	0.7	593, 489, 417, 285	Isosakuranetin-O-rutinoside derivative	*	*		*	Flav.
80	281.4	282, 322	$C_{23}H_{39}O_9$	459.26	0.9	439, 417, 359, 297	Unidentified				*	
81	282.7	272 sh, 322 sh	$C_{28}H_{33}O_{14}$	593.2	1.9	443, 285	Isosakuranetin-O-rutinoside			*		Flav.
82	283.8	283, 325 sh	$C_{28}H_{33}O_{15}$	609.18	0.8	441, 301	Hesperidin isomer				*	Flav.
83	285.8	276, 320	$C_{40}H_{51}O_{25}$	931.27	1.8	785, 667, 623, 591, 489, 417, 299	Diosmetin-di-hexose-rutinoside		*			Flav.
84	286.8	270 sh, 325 sh, 366 sh	$C_{35}H_{39}O_{21}$	795.2	0.1	765, 737, 693, 235	Unidentified			*		
85	288.8	268 sh, 315 sh, 366 sh	$C_{17}H_{17}O_8$	349	3.5	231, 201	Unidentified			*		
86	292.5	276, 322, 345 sh	$C_{20}H_{17}O_{10}$	417.08	3.7	355, 327, 295, 285, 250, 243	Kaempferol-O-pentoside	*	*			Flav.
87	293.2	280, 323	$C_{31}H_{49}O_9$	565.33	3.4	417,295	Unidentified				*	
88	295.5	270 sh, 315 sh	$C_{26}H_{29}O_{10}$	501.17	1.9	401, 339, 269, 267, 201	Methylbutenyl-apigenin-O-hexoside {Flavaprin}			*		Flav.
89	297.9	270 sh, 315 sh, 365 sh	$C_{13}H_{13}O_6$	265.07	0.2	221	Hydroxy-trimethoxy-methylchromen-4-one			*		Coum.
90	298.3	278, 316 sh	$C_{35}H_{51}O_{15}$	711.32	7.7	649, 575, 503, 491, 479	Unidentified		*			
91	302.9	282 sh, 320, 345	$C_{36}H_{33}O_{17}$	737.17	1.2	707, 613, 543, 417, 355	Unidentified	*				
92	303	280, 324, 345 sh	$C_{20}H_{17}O_{10}$	417.08	1.1	355, 295, 285, 251, 243	Kaempferol-O-pentoside isomer				*	Flav.
93	305.3	268 sh, 325 sh	$C_{17}H_{29}O_8$	361.18	0.1	315, 199	Unknown acid			*		
94	307.3	274, 325	$C_{33}H_{39}O_{18}$	723.21	0.3	621, 579, 433, 271	Melitidin {Naringenin-7-[2″-rhamnosyl-6″-[3″“hydroxy-3″”-methylglutaryl]-glucoside]}	*	*		*	Flav.
95	308.7	268 sh, 315 sh	$C_{26}H_{35}O_{11}$	523.21	0.2	451, 361, 245	Unknown fatty acid			*		F.A.
96	310.4	275, 324	$C_{35}H_{47}O_{14}$	691.29	0.4	643, 575, 449, 248, 161	Unidentified		*			
97	312.7	286, 324	$C_{15}H_{11}O_5$	271.06	2.5	161	Naringenin aglycone				*	Flav.
98	313	286, 325	$C_{18}H_{31}O_5$	327.21	0.6	271, 161	Trihydroxy-octadecadienoic acid (C18:2)	*	*		*	F.A.
99	313.1	268 sh, 320 sh	$C_{37}H_{61}O_{18}$	793.3	1.1	661, 639, 593, 327,243, 201	Isosakuranetin-O-rutinoside derivative			*		Flav.
100	316.4	268 sh, 310 sh	$C_{35}H_{29}O_6$	545.2	4.2	523, 487, 459, 395, 327	Unidentified			*		
101	318.1	316 sh	$C_{16}H_{11}O_7$	315.05	0.7	300	Methoxy-tetrahydroxyflavone {isorhamnetin aglycone}			*		Flav.
102	318.8	286, 323	$C_{33}H_{29}O_{15}$	665.15	1	543, 499, 357, 299, 161	Diosmetin derivative	*	*		*	Flav.
103	320.1	337 sh	$C_{16}H_{11}O_6$	299.05	2.4	248, 161	Diosmetin aglycone	*	*			Flav.
104	320.5	268 sh, 320 sh	$C_{18}H_{29}O_7$	357.18	7.1	327, 315, 299, 221	Isorhamnetin derivative			*		Flav.
105	325.2	330 sh, 370 sh	$C_{17}H_{13}O_8$	345.06	1.1	315, 221	Tetrahydroxy-dimethoxyflavone			*		PMF
106	325.5	323	$C_{30}H_{39}O_{10}$	559.25	0.5	533, 441, 345,315	Isorhamnetin aglycone derivative				*	Flav.
107	329.5	273, 328	$C_{18}H_{33}O_5$	329.23	0.1	286, 161	Trihydroxy-octadecenoic acid (C18:1)	*	*	*	*	F.A.
108	331.9	322, 346	$C_{36}H_{63}O_{16}$	751.41	0.9	665, 579, 397, 329	Unidentified				*	
109	335.6	274 sh, 331, 346	$C_{20}H_{25}O_7$	377.16	1.2	329, 286, 248, 161	Unknown diterpene	*			*	Terp.
110	342.2	325 sh	$C_{21}H_{25}O_8$	405.15	1.9	369, 327, 287, 229	Unknown diterpene			*		Terp.
111	345.4	Nd	$C_{18}H_{29}O_5$	325.2	1.4	248, 211	Trihydroxy-octadecatrienoic acid (18:3)	*				F.A.
112	350.8	Nd	$C_{18}H_{31}O_5$	327.21	1.8	248, 221, 161	Trihydroxy-octadecadienoic acid (C18:2)	*	*			F.A.
113	354.1	266, 310 sh	$C_{22}H_{33}O_9$	441.21	1.8	395, 285, 237	Unidentified			*		
114	356.2	271, 318, 345	$C_{17}H_{13}O_6$	313.07	2.9	298, 283, 276, 248, 242, 161	Dihydroxy-dimethoxyflavone		*			PMF
115	357.2	321, 346	$C_{30}H_{39}O_{13}$	607.23	0.7	579, 517, 441, 371, 313	Unidentified				*	

(*Continued*)

Table I. Continued

Peak	Rt (s)	UV (nm)	Deprotonated molecular formula	Mol. Ion $[M-H]^-$ *m/z* (-)	Error *m/z* (ppm)	MSn ions *m/z* (-) MS–MS	Identification	CR	CS	CA	CP	Class
116	359.2	265, 330	$C_{18}H_{33}O_5$	329.23	2.6	211, 161	Trihydroxy-octadecenoic acid (C18:1)		*			F.A.
117	359.5	256, 321	$C_{14}H_{13}O_3$	229.08	0.4	211, 203, 161	Unidentified			*	*	
118	361.9	Nd	$C_{18}H_{31}O_5$	327.21	2.6	248, 221, 161	Trihydroxy-octadecadienoic acid (C18:2) isomer	*				F.A.
119	364.9	267, 331, 345	$C_{18}H_{15}O_7$	343.08	1.1	328, 295, 249, 161	Dihydroxy-trimethoxyflavone		*			PMF
120	367	264sh, 309	$C_{22}H_{25}O_8$	417.15	0.7	371, 201	Unidentified				*	
121	371.3	Nd	$C_{13}H_{19}O_3$	223.13	2.5	208, 180, 174, 161	Unidentified terpene	*				Terp.
122	375.7	266, 328 sh	$C_{18}H_{15}O_7$	343.08	2.7	325, 311, 248	Dihydroxy-trimethoxyflavone isomer	*				PMF
123	380.7	277, 331 sh, 346	$C_{16}H_{13}O_5$	285.07	1	269, 242, 174, 161	Dihydroxy-methoxyflavanone	*				PMF
124	383.8	289, 332	$C_{19}H_{17}O_8$	373.09	3.1	358, 343, 328, 325, 307, 289	Dihydroxy-tetramethoxyflavone	*	*		*	PMF
125	388.2	266, 327	$C_{20}H_{19}O_8$	387.1	0.3	329, 326, 311, 248, 161	Hydroxy-pentamethoxyflavone		*			PMF
126	390.5	323, 345	$C_{17}H_{25}O_4$	293.17	0	248, 229, 174, 161	Unidentified	*			*	
127	391.5	267 sh, 300 sh, 346	$C_{14}H_{13}O_3$	229.08	3.4	201, 180, 174, 161	Allyloxy-dimethylcoumarin			*		Coum.
128	405	323, 345	$C_{18}H_{29}O_4$	309.2	0.9	248, 161	Dihydroxy-octadecatrienoic acid				*	F.A.
129	409.7	271, 322	$C_{18}H_{29}O_4$	309.2	1.5	248, 161	Dihydroxy-octadecatrienoic acid isomer	*	*	*		F.A.
130	424.2	300 sh, 346	$C_{27}H_{41}O_{11}$	541.26	2.7	415, 325, 311	Unidentified			*		
131	429	Nd	$C_{18}H_{31}O_4$	311.22	0.3	248, 201, 161	Dihydroxy-octadecadienoic acid	*	*	*	*	F.A.
132	436	Nd	$C_{18}H_{31}O_4$	311.22	0.7	248, 161	Dihydroxy-octadecadienoic acid isomer	*	*	*		F.A.
133	440.4	266 sh, 315 sh, 346	$C_{18}H_{27}O_4$	307.19	0.5	289, 277	Dihydroxy-octadecatetraenoic acid	*	*	*		F.A.
134	444	Nd	$C_{18}H_{27}O_3$	291.19	0.1	265, 248, 161	Hydroxy-octadecatetraenoic acid	*	*			F.A.
135	451.1	Nd	$C_{15}H_{21}O_4$	265.14	13	201, 161	Unknown sesquiterpene	*	*	*	*	Misc.
136	454.8	Nd	$C_{19}H_{21}O_3$	297.14	9.6	265, 161	Auraptene {O-Geranylumbelliferone}	*	*			Coum.
137	456.2	Nd	$C_{18}H_{29}O_3$	293.21	0.8	275, 265	Hydroxy-octadecatrienoic acid	*		*	*	F.A.
138	461.3	Nd	$C_{34}H_{43}O_9$	595.29	3.8	564, 261, 293	Unidentified		*			
139	462.3	309 sh	$C_{21}H_{21}O_5$	353.13	0.7	297, 265, 201	Epoxybergamottin {furanocoumarin}				*	Coum.
140	462.9	Nd	$C_{18}H_{29}O_4$	309.2	0.3	297, 293, 265	Dioxo-10-octadecenoic acid	*	*	*		F.A.
141	464.6	309	$C_{19}H_{21}O_3$	297.14	3.4	265, 201, 161	Auraptene isomer				*	Coum.
142	470.7	Nd	$C_{20}H_{23}O_3$	311.16	7.6	297, 265,	Unknown diterpene				*	Terp.
143	484.8	Nd	$C_{18}H_{31}O_3$	295.22	1.7	Nd	Hydroxy-octadecadienoic acid	*	*	*	*	F.A.
144	490.2	Nd	$C_{20}H_{23}O_3$	311.16	8.1	295, 265	Unknown diterpene	*	*			Terp.
145	498.3	Nd	$C_{18}H_{29}O_3$	293.21	2	265	Hydroxy-octadecatrienoic acid isomer	*	*		*	F.A.
146	529.9	Nd	$C_{21}H_{25}O_3$	325.18	10.7	311, 293, 249	Unknown diterpene	*	*	*		Terp.
147	543.8	290 sh, 346	$C_{21}H_{25}O_3$	325.18	14.5	311, 293, 249	Unknown diterpene			*		Terp.
148	561.3	268 sh, 310 sh	$C_{21}H_{35}O_4$	351.25	0.6	325, 307, 231	Unknown fatty acids			*		F.A.
149	569.7	245 sh, 255 sh, 325 sh	$C_{20}H_{23}O_4$	327.16	1.5	248, 191	Unknown fatty acids			*		F.A.
150	572.7	Nd	$C_{16}H_{31}O_3$	271.22	0.8	225	Hydroxy-hexadecanoic acid	*	*	*	*	F.A.
151	577.4	Nd	$C_{18}H_{29}O_2$	277.21	2.9	251, 211	Linolenic acid (18:3)	*	*	*	*	F.A.
152	584.5	310 sh, 346	$C_{32}H_{49}O_9$	577.33	4.6	423, 339	Unidentified			*		
153	594.3	Nd	$C_{16}H_{29}O_2$	253.21	0.3	171, 161	Hexadecenoic acid {Palmitoleic acid}	*				F.A.

(*Continued*)

Table I. Continued

Peak	Rt (s)	UV (nm)	Deprotonated molecular formula	Mol. Ion $[M-H]^-$ m/z (-)	Error m/z (ppm)	MSn ions m/z (-) MS–MS	Identification	CR	CS	CA	CP	Class
154	601.7	Nd	$C_{25}H_{47}O_9$	491.32	5.4	389, 339,325, 321, 311, 253	Hydroxy-hexaoxaicosyl-undecenoate				*	F.A.
155	610.4	Nd	$C_{18}H_{31}O_2$	279.23	2.1	211	Linoleic acid (18:2)	*	*	*	*	F.A.
156	620.5	300 sh, 346	$C_{26}H_{49}O_9$	505.33	3.1	391, 325, 311, 279	Dodecanoic acid, pentaester with triglycerol			*		F.A.
157	638	Nd	$C_{16}H_{31}O_2$	255.23	2.7	Nd	Palmitic acid (16:0)	*	*	*	*	F.A.
158	646.8	Nd	$C_{18}H_{33}O_2$	281.24	0	Nd	Oleic acid (16:1)	*	*	*	*	F.A.
159	656.2	Nd	$C_{17}H_{33}O_2$	269.24	0.6	182	Methylhexadecanoic acid			*	*	F.A.
160	663.3	Nd	$C_{17}H_{33}O_2$	269.24	1.2	182	Methylhexadecanoic acid isomer	*		*	*	F.A.
161	684.2	Nd	$C_{24}H_{47}O_3$	383.35	2.1	325, 311	Hydroxytetracosanoic acid	*	*		*	F.A.
162	663.7	Nd	$C_{24}H_{47}O_3$	383.35	0.5	325, 311	Hydroxytetracosanoic acid isomer				*	F.A.
163	688.3	Nd	$C_{18}H_{35}O_2$	283.26	3.3	Nd	Stearic acid (18:0)			*	*	F.A.

Note: CR (*C. reticulata* Blanco cv. Egyptian); CS (*C. sinensis* L. Osbeck cv. Olinda Valencia); CA (*C. aurantiifolia* Swingle cv. Mexican); CP (*C. paradisi* Macfad. cv. Duncan); Misc. (Miscellaneous); Cinn.a. (Cinnamic acid conjugate); Coum. (Coumarin); PMF (Polymethoxyflavone); Flav. (Flavonoid); Terp. (Terpene); F.A. (Fatty ac).

Peaks (136 and 139), $[M-H]^-$ at m/z 297.14 $(C_{19}H_{21}O_3)^-$ and at m/z 353.13 $(C_{21}H_{21}O_5)^-$ were assigned as auraptene and epoxybergamottin, respectively, previously reported in *C. aurantiifolia* and *C. paradise* (34, 35).

Identification of *C/O*-flavonoids

Flavonoid glycosidic conjugates represented the most abundant class in *Citrus* species. They were eluted in the second part of the chromatographic run (Rt 211–350 s) as evidenced from their two distinct λ_{max} at 270 and 325–350 nm. MS–MS was performed to assist in *O*-glycosides structural elucidation, where the nature of sugars in *O*-glycosides could be distinguished from elimination of the sugar residue from molecular ions, i.e., 162 amu (hexose; glucose or galactose), 146 amu (deoxyhexose), 132 amu (pentose) or 130 (dideoxyhexose) (36). Another fragmentation pattern was also observed in *C*-flavonoids including the loss of water $[M-18]^-$ and cross-ring cleavages [(O-C1 and C2-C3)] or [(O-C1 and C3-C4)] of the sugar units, namely, $[M-120/90]^-$ for *C*-hexosides, $[M-90/60]^-$ for *C*-pentosides and $[M-104/74]^-$ for *C*-deoxyhexosides (37, 38).

C-flavonoids

The fragmentation pattern of flavone-di-*C*-glycoside [M-90/ 120/ 210]$^-$ was clearly observed in MS spectrum of peaks (34 and 42) with a respective $[M-H]^-$ m/z 579.13 $(C_{26}H_{27}O_{15})^-$ and $[M-H]^-$ m/z 593.16 $(C_{27}H_{29}O_{15})^-$. These peaks (34 and 42) were identified as luteolin-*C*-hexoside-*C*-pentoside (39) and apigenin-di-*C*-hexoside {Vicenin-2}, respectively. Vicenin-2 was previously detected in *C. aurantiifolia* (40). Peak (78), $[M-H]^-$ at m/z 417.08 $(C_{20}H_{17}O_{10})^-$, with fragment ion at m/z 327 $[M-90-H]^-$ was annotated as luteolin-*C*-pentoside (39). It is worth to note that both luteolin-*C*-glycosides (peaks 34 and 78) are first to be reported in *Citrus* peels.

O-flavonoids

In contrast to *C*-glycosides that give rise to non-homogenous fragments, the readily cleaved sugar moieties from aglycone infers *O*-type glycosides and found in most identified flavonol peaks. In flavone-*O*-glycoside, a common loss of 162 amu observed in peaks (37 and 88), $[M-H]^-$ at *m/z* 593.15 $(C_{27}H_{29}O_{15})^-$ and $[M-H]^-$ at m/z 501.20 $(C_{26}H_{29}O_{10})^-$ annotated as vitexin-2″-*O*-hexoside (41) and methylbutenyl-apigenin-*O*-hexoside {Flavaprin} (42), respectively. The loss of 132 amu for loss of pentose moiety evident in peaks (40, 86 and 92), $[M-H]^-$ at m/z 563.14 $(C_{26}H_{27}O_{14})^-$, 417.10 $(C_{20}H_{17}O_{10})^-$ and 417.10 $(C_{20}H_{17}O_{10})$ were assigned as vitexin-*O*-pentoside (43), kaempferol-*O*-pentoside (44) and its isomer, respectively. All of these *O*-glycosides in peaks 37, 40, 86, 88 and 92 are first time to be reported in *Citrus* peels.

A typical fragmentation pattern of flavone-di-*O*-glucoside was observed in several peaks (47, 51, 54, 55, 56, 57, 79, 81, 82 and 99), where a product ion of $[M-308-H]^-$ indicative for the loss of rutinoside moiety have been observed. Similar parent ion (m/z 593.2) observed as product ion in both peaks (79 and 99) with a $[M-H]^-$ at m/z 639.20 $(C_{29}H_{35}O_{16})^-$ and m/z 793.30 $(C_{37}H_{16}O_{18})^-$, besides other fragment ions at m/z 285 and m/z 243, respectively, and annotated as isosakuranetin-*O*-rutinoside derivatives, first to be reported in *Citrus* peels. A common loss of 324 amu, indicating dihexose moiety, have been appeared in peak (83) which exhibited $[M-H]^-$ at m/z m/z 931.30 $(C_{40}H_{51}O_{25})^-$, besides other fragment

ion at m/z 299, and was identified as diosmetin-di-hexose-rutinoside, which is reported for the first time in *Citrus* peels.

Acyl sugar derivatives including acetyl derivatives were identified in peaks (63, 72, 74 and 75) as evident from the sequential loss of 42 amu. Peaks (63, 72 and 74) were characterized by an $[M-H]^-$ m/z 489.10 $(C_{23}H_{21}O_{12})^-$, product ions m/z 285 $[M-162-H]^-$ and identified as luteolin-acetyl hexoside and its isomers (45). Same parent ion m/z 489.10 appeared as product ion in peak (73), $[M-H]^-$ m/z 669.20 $(C_{30}H_{37}O_{17})^-$, and annotated as luteolin-acetyl hexoside derivative. An extra 162 amu unit than in peak (63) was observed in peak (75), $[M-H]^-$ at m/z 651.16 $(C_{29}H_{31}O_{17})^-$, and product ions at *m/z* 285, and assigned as kaempferol-dihexosyl acetate (46). The previously detected parent ion at m/z 651.16 was detected as fragment ion in peak (77), $[M-H]^-$ m/z 707.22 $(C_{33}H_{39}O_{17})^-$, with an extra 56 amu indicating the presence of butyl group, so peak (77) was identified as kaempferol-dihexosyl butyl acetate. It is worth to note that all the detected acyl sugar derivatives of luteolin and kaempferol (peaks 63, 72–75 and 77) are first to be reported in *Citrus* peels.

Identification of polymethoxyflavones

It should be noted that PMFs are found almost exclusively in *Citrus* species (47). The peaks of PMFs in the base peak ion chromatogram were more easily seen in the positive ion mode than that in the negative ion mode. In the MS^2 spectrum, PMFs have characteristic fragmentations. They could form the diagnostic fragments of $[M + H\text{-}nCH_3]^+$, $[M + H\text{-}2CH_3\text{-}H_2O]^+$ and $[M + H\text{-}2CH_3\text{-}CO]^+$ (48, 49). A typical fragmentation pattern of PMFs has been noticed in several peaks (105, 114, 119, 122, 123, 124 and 125). These peaks were identified as tetrahydroxy-dimethoxyflavone, dihydroxy-dimethoxyflavone, dihydroxy-trimethoxyflavone, dihydroxy-trimethoxyflavone isomer, dihydroxy-methoxyflavanone, dihydroxy-tetramethoxyflavone and hydroxy-pentamethoxyflavone, respectively. It is worth to note that all of the listed PMFs were previously reported in *Citrus* peels (50, 51), except dihydroxy-methoxyflavanone which was previously reported in *Citrus* juice (52) and for the first time to be detected in *C. reticulate* peels.

Identification of fatty acid conjugates

In the third part of the chromatographic run (Rt 350–800 s), the ESI–MS spectra revealed the presence of several fatty acids, most abundant in *C. reticulata* and *C. aurantiifolia* extracts. Saturated fatty acids with methylated group were observed. Both peaks 159 and 160, m/z 269.24 $(C_{17}H_{33}O_2)^-$ were identified as methylated hexadecanoic acid and its isomer, respectively.

Several hydroxylated fatty acids were also identified in peaks (131 and 132) [m/z 311.22 $(C_{18}H_{31}O_4)^-$], (128 and 129) [m/z 309.2 $(C_{18}H_{29}O_4)^-$] and (133) [m/z 307.19 $(C_{18}H_{27}O_4)^-$] were assigned as dihydroxy-octadecadienoic acid and its isomer, dihydroxy-octadecatrienoic acid and its isomer and dihydroxy-octadecatetraenoic acid, respectively. Likewise, the three sets of peaks (111) [m/z 325.2 $(C_{18}H_{29}O_5)^-$], (112 and 118) [m/z 327.21 $(C_{18}H_{31}O_5)^-$] and (116) [m/z 329.23 $(C_{18}H_{33}O_5)^-$] were identified as trihydroxy-octadecatrienoic acid, trihydroxy-octadecadienoic acid and its isomer and trihydroxy-octadecenoic acid, respectively. The other peaks (150) [m/z 271.22 $(C_{16}H_{31}O_3)^-$] and (161 and 162) [m/z 383.35 $(C_{24}H_{47}O_3)^-$] were assigned as hydroxy-hexadecanoic acid and hydroxytetracosanoic acid and its isomer, respectively. Additionally, peak (134) [m/z 291.19 $(C_{18}H_{27}O_3)^-$] was assigned as hydroxy-octadecatetraenoic acid (53). This is the first report for the presence of oxygenated fatty acids and methylated fatty acids in *Citrus* species and suggests that UPLC–MS represents a useful technology and another platform for fatty acids profiling in *Citrus* spp. There is an increasing interest in hydroxylated fatty acids due to their anti-inflammatory, antimicrobial and cytotoxic activities (54, 55).

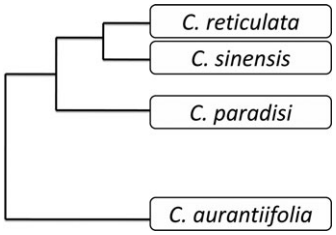

Figure 2. Hierarchical cluster analysis (HCA) dendrogram of the four tested Citrus peels analyzed by UPLC–qTOF–MS.

Unsupervised multivariate data analysis of *Citrus* metabolite profiles *via* UPLC–MS

Although different metabolite patterns were revealed by visual inspection of UPLC–MS traces from different *Citrus* specimens (Figure 1), HCA was attempted as a more holistic approach to explore the relative variability within *Citrus* peels. HCA is an unsupervised clustering method, requiring no knowledge of the data set and act to reduce the dimensionality of multivariate data and are increasingly applied for the analysis of herbal drugs (56).

Hierarchical cluster analysis

In terms of chemical composition, the tight clustering of *C. reticulate and C. sinensis* peels suggests that they share comparable secondary metabolite profile and are closer in chemical composition than that of *C. paradisi*. *C. aurantiifolia* appeared as the most distant from the all tested *Citrus* peels. Heat density plot revealed that MS signals of flavonol glycosides as naringin, isosakuranetin-*O*-rutinoside, isosakuranetin-*O*-rutinoside derivatives, luteolin-acetyl hexoside were more enriched in *C. reticulata*, *C. sinensis* and *C. paradisi* peels. Enrichment of these flavonoids is in agreement with total flavonoid assay results in *C. reticulata*, *C. sinensis* and *C. paradisi* peels (Figure 2). In contrast, MS signals of cinnamic acid conjugates, i.e., dihydroxycinnamic acid hexoside, dimer of dihydroxycinnamic acid hexoside were found more abundant in *C. aurantiifolia* peels (data not shown).

Conclusion

This study presents the first comprehensive report for the compositional difference among four *Citrus* peels *via* a metabolomic approach using UPLC–qTOF–MS technique. It is worth noting that it provides a comprehensive metabolite profile of *Citrus* peels species containing such a large number of compounds; a total of 163 peaks were characterized, in peels of the four *Citrus* species [*C. reticulata* Blanco cv. Egyptian, *C. sinensis* (L.) Osbeck cv. Olinda Valencia, *C. aurantiifolia* Swingle cv. Mexican and *C. paradisi* Macfad. cv. Duncan]. To the best of our knowledge, 28 compounds were detected for the first time in these cultivars (Table II) including eight coumarin derivatives, three cinnamic acids conjugates, one PMF, five *O*-glycosides, two *C*-glycosides, three flavone-di-*O*-glucosides and six acetyl sugar derivatives of luteolin and kaempferol in addition to oxygenated and methylated fatty acids. Flavonoids amounted

Table II. List of the Compounds Detected for the First Time in the Four Studied *Citrus* Peels Cultivars

Peak	Identification	Class
10	Trihydroxycoumarin hexoside	Coumarin
11	Trihydroxycoumarin hexoside isomer	Coumarin
12	Methoxy-trihydroxycoumarin hexoside	Coumarin
14	Methoxy-trihydroxycoumarin hexoside isomer	Coumarin
18	Methoxy-umbelliferone-hexoside	Coumarin
23	Methoxy-trihydroxycoumarin hexoside isomer	Coumarin
25	Dimethoxy-umbelliferone hexoside	Coumarin
28	Benzyl-methyl-cyclohexanecarboxylate-umbelliferone pentoside	Coumarin
31	Dihydroxyhydrocinnamic acid hexoside	Cinnamic acid conjugate
32	Dimer of Dihydroxyhydrocinnamic acid hexoside	Cinnamic acid conjugate
34	Luteolin-*C*-hexoside-*C*-pentoside	Flavonoid-*C*-glycosides
37	Vitexin-2″-*O*- hexoside	Flavonoid-*O*-glycosides
40	Vitexin-*O*-pentoside	Flavonoid-*O*-glycosides
49	Feruloyl rutinoside	Cinnamic acid conjugate
63	Luteolin-acetyl hexoside	Flavonoid
72	Luteolin-acetyl hexoside isomer	Flavonoid
73	Luteolin-acetyl hexoside derivative	Flavonoid
74	Luteolin-acetyl hexoside isomer	Flavonoid
75	Kaempferol-dihexosyl acetate	Flavonoid
77	Kaempferol-dihexosyl butyl acetate	Flavonoid
78	Luteolin-*C*-pentoside	Flavonoid-*C*-glycosides
79	Isosakuranetin-*O*-rutinoside derivative	Flavone-di-*O*-glucoside
83	Diosmetin-di-hexose-rutinoside	Flavone-di-*O*-glucoside
86	Kaempferol-*O*-pentoside	Flavonoid-*O*-glycosides
88	Methylbutenyl-apigenin-*O*-hexoside {Flavaprin}	Flavonoid-*O*-glycosides
92	Kaempferol-*O*-pentoside isomer	Flavonoid-*O*-glycosides
99	Isosakuranetin-*O*-rutinoside derivative	Flavone-di-*O*-glucoside
123	Dihydroxy-methoxyflavanone	PMF

for the most abundant secondary metabolites class in *Citrus* peels. The predominant flavones were glycosides of luteolin and kaempferol as well as naringenin conjugates, whereas trihydroxycoumarin hexoside was the main coumarin conjugate. Flavonoids were found more enriched in the *C. reticulata*, *C. sinensis* and *C. paradisi* peels, and contributed the most to the discrimination between them. Furthermore, the chemical composition of the *C. reticulata*, *C. sinensis* and *C. paradise* peels were found to be similar than that of *C. aurantiifolia* peels. Such data with respect to *Citrus* peels metabolite profiling could coordinate in figuring out which *Citrus* peels ought to be prioritized for future domestication and agricultural advancement which may energize its utilization as functional foods.

Acknowledgments

The authors are sincerely gratitude for Prof. Dr Ludger A. Wessjohann, Department of Bioorganic Chemistry, Leibniz Institute of Plant Biochemistry, Weinberg, Halle Salle, Germany, for assistance in analyzing the samples using UPLC–MS.

Funding

Dr Mohamed Farag acknowledges the funding received from the Alexander von Humboldt foundation, Germany to his laboratory at Cairo University and the American University in Cairo (AUC) internal research grant support.

References

1. Wolfender, J.L., Rudaz, S., Choi, Y.H., Kim, H.K.; Plant metabolomics: from holistic data to relevant biomarkers; *Current Medical Chemistry*, (2013); 20(8): 1056–1090.
2. Farag, M.A., El-Ahmady, S.H., Elian, F.S., Wessjohann, L.A.; Metabolomics driven analysis of artichoke leaf and its commercial products *via* UHPLC-q-TOF-MS and chemometrics; *Phytochemistry*, (2013); 95: 177–187.
3. Okada, T., Nakamura, Y., Kanaya, S., Takano, A., Malla, K.J., Nakane, T., *et al.*; Metabolome analysis of *Ephedra* plants with different contents of ephedrine alkaloids by using UPLC-Q-TOF-MSl; *Planta Medica*, (2009); 75: 1356–1362.
4. Hanhineva, K., Soininen, P., Anttonen, M.J., Kokko, H., Rogachev, I., Aharoni, A., *et al.*; NMR and UPLC-qTOF-MS/MS characterisation of novel phenylethanol derivatives of phenylpropanoid glucosides from the leaves of strawberry (*Fragaria* × *ananassa* cv. Jonsok); *Phytochemical Analysis*, (2003); 20: 353–364.
5. Davies, F.S., Albrigo, L.G.; *Citrus*, Vol. 1. CAB International, Wallingford, (1994).
6. Laufenberg, G., Kunz, B., Nystroem, M.; Transformation of vegetable waste into value added products: (A) the upgrading concept; (B) practical implementations; *Bioresource Technology*, (2003); 87(2): 167–198.
7. Andrea, V., Nadia, N., Teresa, R.M., Andrea, A.; Analysis of some Italian lemon liquors (*Limoncello*); *Journal of Agriculture and Food Chemistry*, (2003); 51(17): 4978–4983.
8. González-Molina, E., Domínguez-Perles, R., Moreno, D.A., GarcíaViguera, C.; Natural bioactive compounds of *Citrus* limon for food and health; *Journal of Pharmaceutical and Biomedical Analysis*, (2010); 51(2): 327–345.
9. Rafiq, S., Kaul, R., Sofi, S.A., Bashir, N., Nazir, F., Nayik, G.A.; *Citrus* peel as a source of functional ingredient: a review; *Journal of the Saudi Society of Agriculture Science*, (2018); 17(4): 351–358.
10. Lin, C.C., Hung, P.F., Ho, S.C.; Heat treatment enhances the NO-suppressing and peroxynitrite-intercepting activities of kumquat (*Fortunella margarita* Swingle) peel; *Food Chemistry*, (2008); 109(1): 95–103.
11. Murakami, A., Nakamura, Y., Ohto, Y., Yano, M., Koshiba, T., Koshimizu, K.; Suppressive effects of *Citrus* fruits on free radical

generation and nobiletin, an anti-inflammatory polymethoxy flavonoid; *Biofactors (Oxford, England)*, (2000); 12: 187–192.
12. Dhanavade, M.J., Jalkute, C.B., Ghosh, J.S., Sonawane, K.D.; Study antimicrobial activity of lemon (*Citrus lemon* L.) peel extract; *British Journal of Pharmacology and Toxicology*, (2011); 2: 119–122.
13. Bok, S.H., Lee, S.H., Park, Y.B., Bae, K.H., Son, K.H., Jeong, T.S., *et al*.; Plasma and hepatic cholesterol and hepatic activities of 3-hydroxy-3-methyl-glutaryl-CoA reductase and acyl CoA: cholesterol transferase are lower in rats fed *Citrus* peel extract or a mixture of *Citrus* bioflavonoids; *Journal of Nutrition*, (1999); 129: 1182–1185.
14. Wilcox, L.J., Borradaile, N.M., de Dreu, L.E., Huff, M.W.; Secretion of hepatocyte apoB is inhibited by the flavonoids, naringenin and hesperetin, via reduced activity and expression of ACAT2 and MTP; *Journal of Lipid Research*, (2001); 42: 725–734.
15. Whitman, S.C., Kurowska, E.M., Manthey, J.A., Daugherty, A.; Nobiletin, a *Citrus* flavonoid isolated from tangerines, selectively inhibits class A scavenger receptor-mediated metabolism of acetylated LDL by mouse macrophages; *Atherosclerosis*, (2005); 178: 25–32.
16. Lee, Y.S., Cha, B.Y., Saito, K., Choi, S.S., Wang, X.X., Choi, B.K., *et al*.; Effects of a *Citrus depressa Hayata* (Skiikuwasa) extract on obesity in high-fat diet-induced obese mice; *Phytomedicine : International Journal of Phytotherapy and Phytopharmacology*, (2011); 18: 6648–6654.
17. Assini, J.M., Mulvihill, E.E., Huff, M.W.; *Citrus* flavonoids and lipid metabolism; *Current Opinion in Lipidology*, (2013); 24: 34–40.
18. Cevallos-Cevallos, J.M., Garcı´a-Torres, R., Etxeberria, E., Reyes- De-Corcuera, J.I.; GC-MS analysis of headspace and liquid extracts for metabolomic differentiation of *Citrus* huanglongbing and zinc deficiency in leaves of 'Valencia' sweet orange from commercial groves; *Phytochemical Analysis*, (2011); 22: 236–246.
19. Yun, Z., Gao, H.J., Liu, P., *et al*.; Comparative proteomic and metabolomic profiling of *Citrus* fruit with enhancement of disease resistance by postharvest heat treatment; *BMC Plant Biology*, (2013); 13(44): 1–16.
20. Pan, Z.Y., Li, Y., Deng, X.X., Xiao, S.Y.; Non-targeted metabolomic analysis of orange (*Citrus sinensis* [L.] Osbeck) wild type and bud mutant fruits by direct analysis in real-time and HPLC-electrospray mass spectrometry; *Metabolomics : Official Journal of the Metabolomic Society*, (2013); 10: 1–16.
21. Frydman, A., Liberman, R., Huhman, D.V., *et al*.; The molecular and enzymatic basis of bitter/non-bitter flavor of *Citrus* fruit: evolution of branch forming rhamnosyltransferases under domestication; *The Plant Journal*, (2013); 73: 166–178.
22. Mehl, F., Marti, G., Boccard, J., *et al*.; Differentiation of lemon essential oil based on volatile and non-volatile fractions with various analytical techniques: a metabolomic approach; *Food Chemistry*, (2014); 143: 325–335.
23. Arbona, V., Iglesias, D.J., Gómez-Cadenas, A.; Non-targeted metabolite profiling of citrus juices as a tool for variety discrimination and metabolite flow analysis; *BMC Plant Biology*, (2015); 15(38): 1–16.
24. Jing, L., Lei, Z., Zhang, G., Pilon, A.C., Huhman, D.V., Xie, R., *et al*.; Metabolite profiles of essential oils in *citrus* peels and their taxonomic implications; *Metabolomics : Official Journal of the Metabolomic Society*, (2015); 11: 952–963.
25. Farag, M.A., Porzel, A., Mahrous, E.A., El-Massry, M.M., Wessjohann, L.A.; Integrated comparative metabolite profiling *via* MS and NMR techniques for Senna drug quality control analysis; *Analytical and Bioanalytical Chemistry*, (2015); 407(7): 1937–1949.
26. Farag, M.A., Handoussa, H., Fekry, M.I., Wessjohann, L.A.; Metabolite profiling in 18 Saudi date palm fruit cultivars and their antioxidant potential *via* UPLC-qTOF-MS and multivariate data analyses; *Food Function*, (2016); 7(2): 1077–1086.
27. Smith, C.A., Want, E.J., Maille, G.O., Abagyan, R., Siuzdak, G.; XCMS: processing mass spectrometry data for metabolite profiling using nonlinear peak alignment, matching, and identification; *Analytical Chemistry*, (2006); 78(3): 779–787.
28. Mabry, T., Markham, K., Thomas, M.; *The Systematic Identification of Flavonoids*. Springer, Berlin, Heidelberg, New York, (1970); pp. 230–270.
29. Ladniya, M.; *Citrus Fruit; Biology, Technology and evaluation*, 1st edn. Academic Press, USA, (2008); p.573.
30. Irkin, R., Dogan, S., Degirmenioglu, N., Diken, M.E., Guldas, M.; Phenolic content, antioxidant activities and stimulatory roles of *Citrus* fruits on some lactic acid bacteria; *Archive of Biolological Science, Belgrade*, (2015); 67(4): 1313–1321.
31..Talapatra, S.K., Talapatra, B.; *Skikimic Acid Pathway. In Chemistry of Plant Natural Products: Stereochemistry, Conformation, Synthesis, Biology and Medicine*. Springer-Verlag, Berlin, Heidelberg, (2015).
32. Jung, M., Zinsmeister, H.D., Geiger, H.Z.; New three- and tetraoxygenated coumarin glucosides from the mosses *Atrichum undulatum* and *Polytrichum formosum*; *Zeitschrift für Naturforschung C*, (1994); 49c: 697–702.
33. Clifford, M.N.; Chlorogenic acids and other cinnamates: nature occurrence, dietary burden, absorption and metabolism; *Journal of the Science of Food and Agriculture*, (2000); 80: 1033–1043.
34. Dugrand, A., Olry, A., Duval, T., Hehn, A., Froelicher, Y., Bourgaud, F.; Coumarin and furanocoumarin quantitation in *Citrus* peel via ultraperformance liquid chromatography coupled with mass spectrometry (UPLC-MS); *Journal of Agriculture and Food Chemistry*, (2013); 61(45): 10677–10684.
35. Dugrand-Judek, A., Olry, A., Hehn, A., Costantino, G., Ollitrault, P., Froelicher, Y., *et al*.; The distribution of coumarins and furanocoumarins in *Citrus* species closely matches *Citrus* phylogeny and reflects the organization of biosynthetic pathways; *PLoS One*, (2015); 10(11): 1–25.
36. Simirgiotis, M.J., Cuevas, H., Tapia, W., Borquez, J.; Edible *Passiflora* (banana passion) fruits: a source of bioactive *C*-glycoside flavonoids obtained by HSCCC and HPLC-DAD-ESI/MS/MS; *Planta Medica*, (2012); 78(11): 1242–1243.
37. Davis, B.D., Brodbelt, J.S.; Determination of the glycosylation site of flavonoid monoglucosides by metal complexation and tandemmass spectrometry; *Journal of the American Society of Mass Spectrometry*, (2004); 15(9): 1287–1299.
38. Figueirinha, A., Paranhos, A., Pérez-Alonso, J.J., Santos-Buelga, C., Batista, M.T.; *Cymbopogon citratus* leaves: characterization of flavonoids by HPLC-PDA-ESI/MS/MS and an approach to their potential as a source of bioactive polyphenols; *Food Chemistry*, (2008); 110(3): 718–728.
39. Roriz, C.L., Barros, L., Carvalho, A.M., Santos-Buelga, C., Ferreira, I.C. F.R.; *Pterospartum tridentatum*, *Gomphrena globosa* and *Cymbopogon citratus*: a phytochemical study focused on antioxidant compounds; *Food Research International*, (2014); 62: 684–693.
40. Brito, A., Ramirez, J.E., Areche, C., Sepúlveda, B., Simirgiotis, M.J.; HPLC-UV-MS profiles of phenolic compounds and antioxidant activity of fruits from three *Citrus* species consumed in Northern Chile; *Molecules (Basel, Switzerland)*, (2014); 19: 17400–17421.
41. Sakalem, M.E., Negri, G., Tabach, R.; Chemical composition of hydroethanolic extracts from five species of the *Passiflora* genus; *Brazilian Journal of Pharmacognosy*, (2012); 22: 1219–1232.
42. Yoo, S.W., Kim, J.S., Kang, S.S., Son, K.H., Chang, H.W., Kim, H.P., *et al*.; Constituents of the fruits and leaves of *Euodia daniellii*; *Archives of Pharmcal Research*, (2002); 25(6): 824–830.
43. Liu, P. Composition of Hawthorn (Crataegus spp.) Fruits and Leaves and Emblic Leafflower (Phyllanthus emblica) Fruits. PH. D., Thesis, Department of Biochemistry and Food Chemistry and Functional Foods Forum, University of Turku, (2012).
44. Simirgiotis, M.J.; Antioxidant capacity and HPLC-DAD-MS profiling of Chilean Peumo (*Cryptocarya alba*) fruits and comparison with German Peumo (*Crataegus monogyna*) from Southern Chile; *Molecules (Basel, Switzerland)*, (2013); 18: 2061–2080.
45. Lee, J.Y., Chang, E.J., Kim, H.J., Park, J.H., Choi, S.W.; Antioxidative flavonoids from leaves of *Carthamus tinctorius*; *Archives of Pharmcal Research*, (2002); 25(3): 313–319.

46. Lim, T.K.; *Edible Medicinal and Non Medicinal Plants, Flowers*, Vol. 8. Springer, Dordrecht, Heidelberg, New York, London, (2014); p.1001.
47. Zheng, G.D., Zhou, P., Yang, H., Li, Y.S., Li, P., Liu, E.H.; Rapid resolution liquid chromatography-electrospray ionization tandem mass spectrometry method for identification of chemical constituents in; *Citri Reticulatae Pericarpium; Food Chemistry*, (2013); 136(2): 604–611.
48. Zhou, D.Y., Xu, Q., Xue, X.Y., Zhang, F.F., Liang, X.M.; Characterization of polymethoxylated flavones in *Fructus aurantii* by off-line two-dimensional liquid chromatography/electrospray ionization-ion trap mass spectrometry; *Journal of Pharmaceutical and Biomedical Analysis*, (2009); 49: 207–213.
49. Zhang, J.Y., Li, N., Che, Y.Y., Zhang, Y., Liang, S.X., Zhao, M.B., *et al.*; Characterization of seventy polymethoxylated flavonoids (PMFs) in the leaves of *Murraya paniculata* by on-line high-performance liquid chromatography coupled to photodiode array detection and electrospray tandem mass spectrometry; *Journal of Pharmaceutical and Biomedical Analysis*, (2011); 56(5): 950–961.
50. Yang, Y., Zhao, X.J., Pana, Y., Zhou, Z.; Identification of the chemical compositions of Ponkan peel by ultra performance liquid chromatography coupled with quadrupole time-of-flight mass spectrometry; *Analytical Methods*, (2016); 8: 893–903.
51. Zhang, H., Xi, W., Zhou, Z., Wang, H.L., Bai, Z.; Bioactivities and structure of polymethoxylated flavones in *Citrus*; *Journal of Food Agriculture and Environment*, (2013); 11(2): 237–242.
52. Gattuso, G., Barreca, D., Gargiulli, C., Leuzzi, U., Caristi, C.; Review: flavonoid composition of *Citrus* juices; *Molecules (Basel, Switzerland)*, (2007); 12: 1641–1673.
53. Elsebai, M.F., Abass, K., Hakkola, J., Atawia, A.R., Farag, M.A.; The wild Egyptian artichoke as a promising functional food for the treatment of hepatitis C virus as revealed *via* UPLC-MS and clinical trials; *Food Function*, (2016); 7(7): 3006–3016.
54. Li, S.S., Jiang, Z.M., Thamm, L., Zhou, G.T.; 10-Hydroxy-2-decenoic acid as an antimicrobial agent in draft keg-conditioned wheat beer; *Journal of American Society of Brewing Chemist*, (2010); 68: 114–118.
55. Martin-Arjol, I., Bassas-Galia, M., Bermudo, E., Garcia, F., Manresa, A.; Identification of oxylipins with antifungal activity by LC-MS/MS from the supernatant of *Pseudomonas* 42A2; *Chemistry and Physics of Lipids*, (2010); 163(4–5): 341–346.
56. Gad, H.A., El-Ahmady, S.H., Abou-Shoer, M.I., Al-Azizi, M.M.; Application of chemometrics in authentication of herbal medicines: a review; *Phytochemical Analysis*, (2013); 24(1): 1–24.